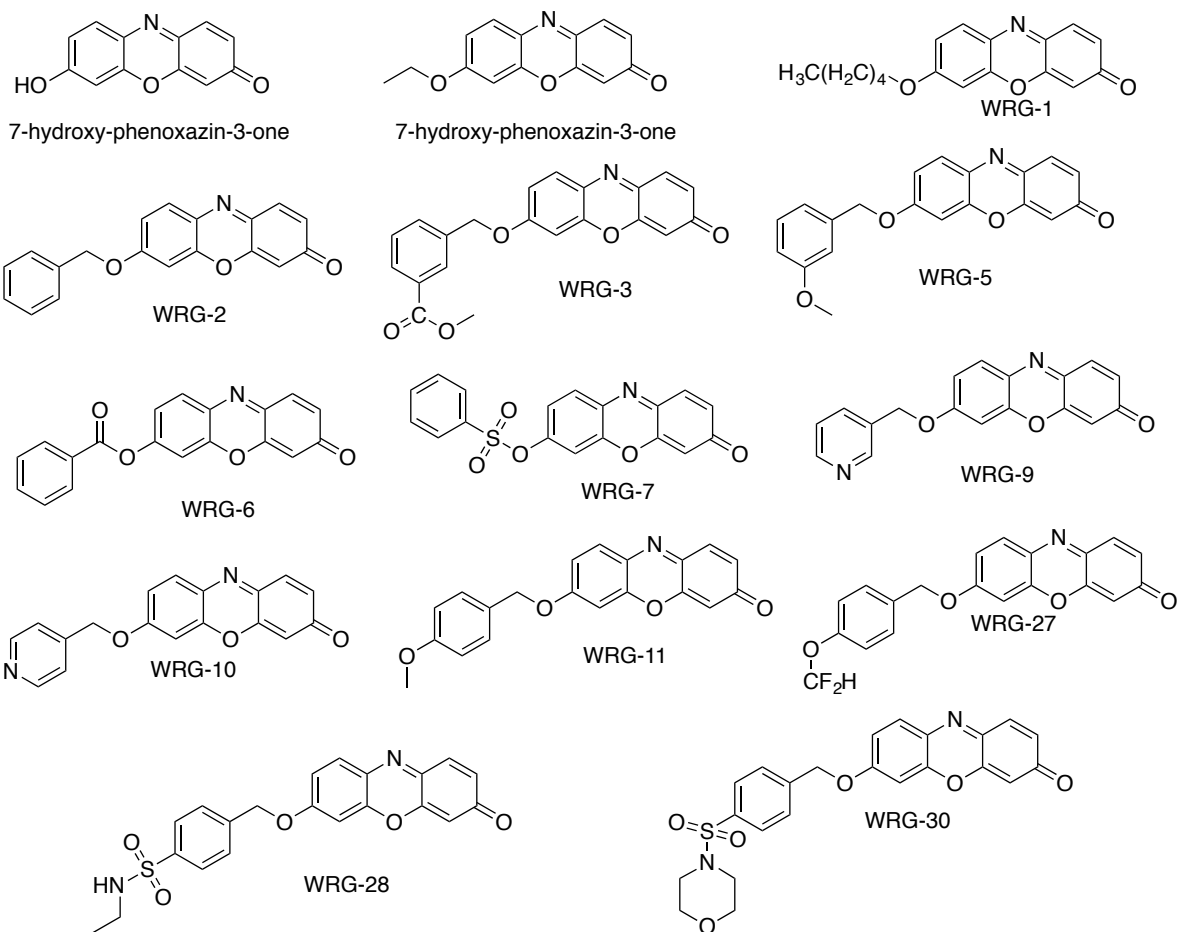


Fig. S1. (A) Solid phase binding assay of 25nM recombinant DDR2-His to the high affinity collagen II DDR2 binding peptide. Graph shows mean \pm SEM from a single experiment representative of at least three independent experiments, three replicates per concentration per experiment. (B) SAR study of the 7-hydroxy-phenoxazin-3-one derivatives and their inhibitory ability as tested by solid phase binding assay of 25nM recombinant DDR2-His to the high affinity collagen II DDR2 binding peptide. Data are mean \pm SEM. IC₅₀ values as determined by 3 independent experiments (n=3). (C) Synthetic route of WRG-28 (a) NET3/CH₂Cl₂; (b) CsCO₃/DMF. (D) MCF10A cell proliferation curve of DMSO control or 1μM WRG-28 treated cells. Means \pm SEM. Three replicates per treatment per experiment. (E) HEK293 cells transfected with DDR1-Myc were added to plates coated with 30μg/mL collagen I for 4 hours in the presence of various concentrations of WRG-28. DDR1 was immunoprecipitated with Myc antibody and bound products western blotted with pTyr mAb 4G10 and reprobed with Myc antibody. Densitometric quantification was performed. Representative blot shown, quantification of 4 independent experiments represented as mean \pm SEM. (F-H) Biolayer interferometry analysis of WRG-28 binding to (F) DDR2-His, (G) DDR2-Fc, (H) DDR1-Fc. Data are shown as black lines representing increasing concentration of WRG-28, with global kinetic fits overlaid. (I) Solid phase binding assays of either 25nM α1β1 integrin (blue) or 25nM DDR2 (green) showing the relative inhibition of binding of each protein to its respective high-affinity triple helical collagen peptide in response to WRG-28. Graph shows mean \pm SEM from a single experiment representative of at least three independent experiments, three replicates per treatment per experiment.



Inactive Derivatives

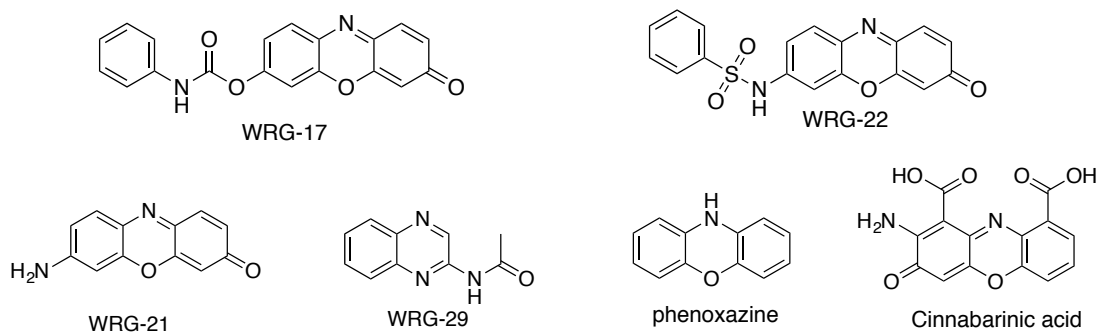


Figure S2. Chemical structures of synthesized derivatives

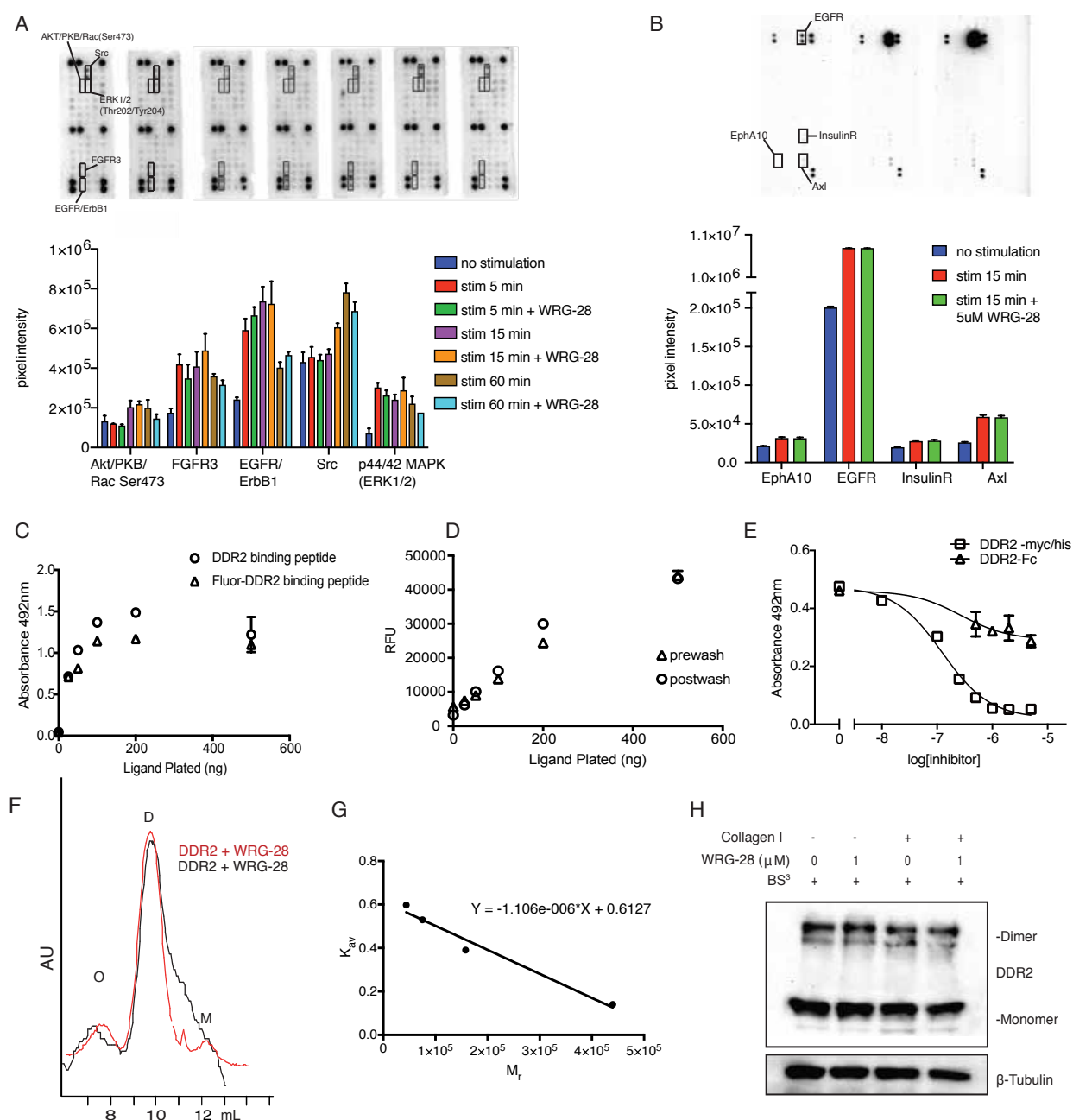


Fig. S3. (A) MCF10A cells were stimulated with 20% horse serum + EGF for indicated time period in the presence or absence of 500nM WRG-28 and cells lysed. Lysates were assayed using Cell Signaling PathScan RTK signaling array. Phosphoarray of RTK signaling pathways shown and graph of mean \pm SEM of select, responsive RTKs in MCF10A cells as quantified by densitometry. (B) MCF10A cells were stimulated with 20% horse serum + EGF for indicated time period in the presence or absence of 5μM WRG-28 and cells lysed. Lysates were assayed using R&D phospho-RTK signaling array. Phosphoarray of RTK signaling pathways shown and graph of mean \pm SEM of select, responsive RTKs in MCF10A cells as quantified by densitometry. (C) Solid phase binding assay of 25nM recombinant DDR2-His to either high affinity DDR2 binding peptide unlabeled or fluorescein conjugated, plated at indicated concentrations. Graph shows mean \pm SEM, three replicates per concentration per experiment. (D) Fluorescein conjugated collagen binding peptide (DDR2 high affinity binding) was plated at known amounts overnight at 4°C. Fluorescence of wells was measured (prewash) and then plating solution washed and fluorescence again measured (postwash) to assess proportion of plated peptide that remained adsorbed to the plate. Graph showing linear adsorption of peptide in the range assessed, with similar fluorescence pre- and post-wash. Three measurements per plating concentration were taken. (E) Effect of WRG-28 on 25ng DDR2-His or DDR2-Fc extracellular domain binding. Inhibitory curves as measured by solid phase binding assay. Graph shows mean \pm SEM from a representative experiment of three independent experiments, three replicates per treatment per experiment. (F) Two independent size exclusion chromatography traces of DDR2-His treated with WRG-28, illustrating the peak shouldering commonly seen. (G) Molecular weight calibration curve of Superdex 200 10/300 GL column using GE Gel Filtration Calibration kit protein standards. Proteins assayed were Ferritin, aldolase, conalbumin, and ovalbumin. Blue dextran 2000 was used to determine the column void volume. Standard curve plotted as shown. (H) HEK293 cells transfected with DDR2-Flag added to plates and stimulated with collagen I in the presence or absence of 1μM WRG-28 for 4 hours. Cells were then treated with 0.1M BS³ in PBS. Samples were western blotted with Myc antibodies. β-tubulin used as a loading control.

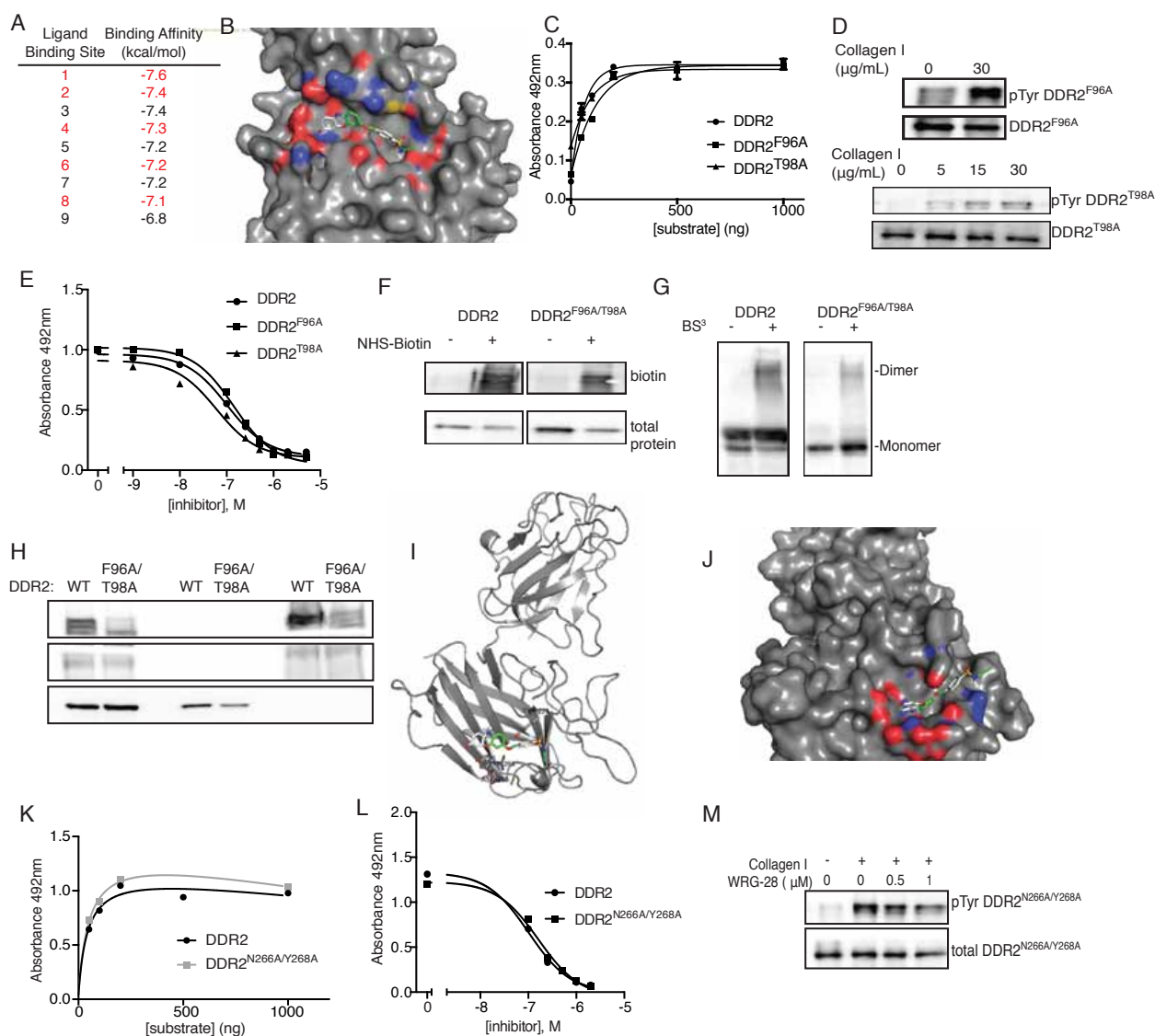


Fig. S4. (A) Autodock calculated binding affinities of top 9 computationally predicted binding sites for WRG-28. Sites highlighted in red represent those clustered within the same site at the DS-DSL interface region. (B) View of WRG-28 oriented in predicted cleft using surface representation of DDR2. Atom colors: nitrogen (blue), oxygen (red), sulfur (yellow). For inhibitor, carbon rendered green. (C) Solid phase binding assay of 25nM recombinant DDR2-His, DDR2F96A-His, or DDR2T98A-His binding to the high affinity DDR2 binding peptide. (D) HEK293 cells transfected with DDR2F96A-Myc or DDR2T98A-Myc were added to plates and stimulated with indicated concentrations of collagen I for 4 hours. Tagged proteins were immunoprecipitated with Myc antibody and bound products western blotted with pTyr 4G10 and then stripped and reprobed with Myc antibodies. (E) Inhibition by WRG-28 of DDR2-His or single point mutants DDR2F96A or DDR2T98A binding. Inhibitory curves as measured by solid phase binding assay of DDR2-His or point mutant binding (25nM). Graph shows mean \pm SEM from a single experiment representative of at least three independent experiments, three replicates per treatment per experiment. (F) Surface biotinylation. Cell surface expression of DDR2-Myc or DDR2F96A/T98A-Myc was confirmed using a biotinylation assay. HEK293 cells expressing indicated constructs were biotinylated using EZ-link NHS-PEG4-Biotin. Proteins were immunoprecipitated using Myc antibody, and then western blotted with Streptavidin-HRP. (G) Cross linking to determine ability of DDR2 constructs to homodimerize. HEK293 cells transfected with DDR2-Myc or DDR2F96A/T98A-Myc were treated with 0.1M BS3 in PBS and analyzed by Western blotting with anti-DDR2 antibody. WT=wild type. (H) Membrane fractionation of DDR2-Myc or DDR2F96A/T98A-Myc to determine cellular localization of proteins. NaK-ATPase was used as a control membrane protein, and tubulin used as control cytosolic protein. Western blotting of proteins in various fractions as shown. (I) Overall view of the DDR2 extracellular domain structure depicting WRG-28 in alternative binding site (Site 3 from S4A). (J) View of WRG-28 oriented in predicted cleft using surface representation of DDR2. For protein and inhibitor atom colors rendered as follows: nitrogen (blue), oxygen (red), sulfur (yellow). For inhibitor, carbon rendered green. (K) Solid phase binding assay of 25nM recombinant DDR2-His or DDR2N266A/Y268A-His binding to the high affinity DDR2 binding peptide. (L) Effect of WRG-28 on DDR2 or DDR2N266A/Y268A extracellular domain binding. Inhibitory curves as measured by solid phase binding assay of DDR2 extracellular domain binding (25nM protein). Graph shows mean \pm SEM from a single experiment representative of at least three independent experiments, three replicates per treatment per experiment. (M) HEK293 cells transfected with DDR2N266A/Y268A-Myc were added to plates coated with 30 μ g/mL collagen I for 4 hours in the presence of various concentrations of WRG-28. DDR2 was immunoprecipitated with Myc antibody and bound products western blotted with pTyr 4G10 or Myc antibodies.

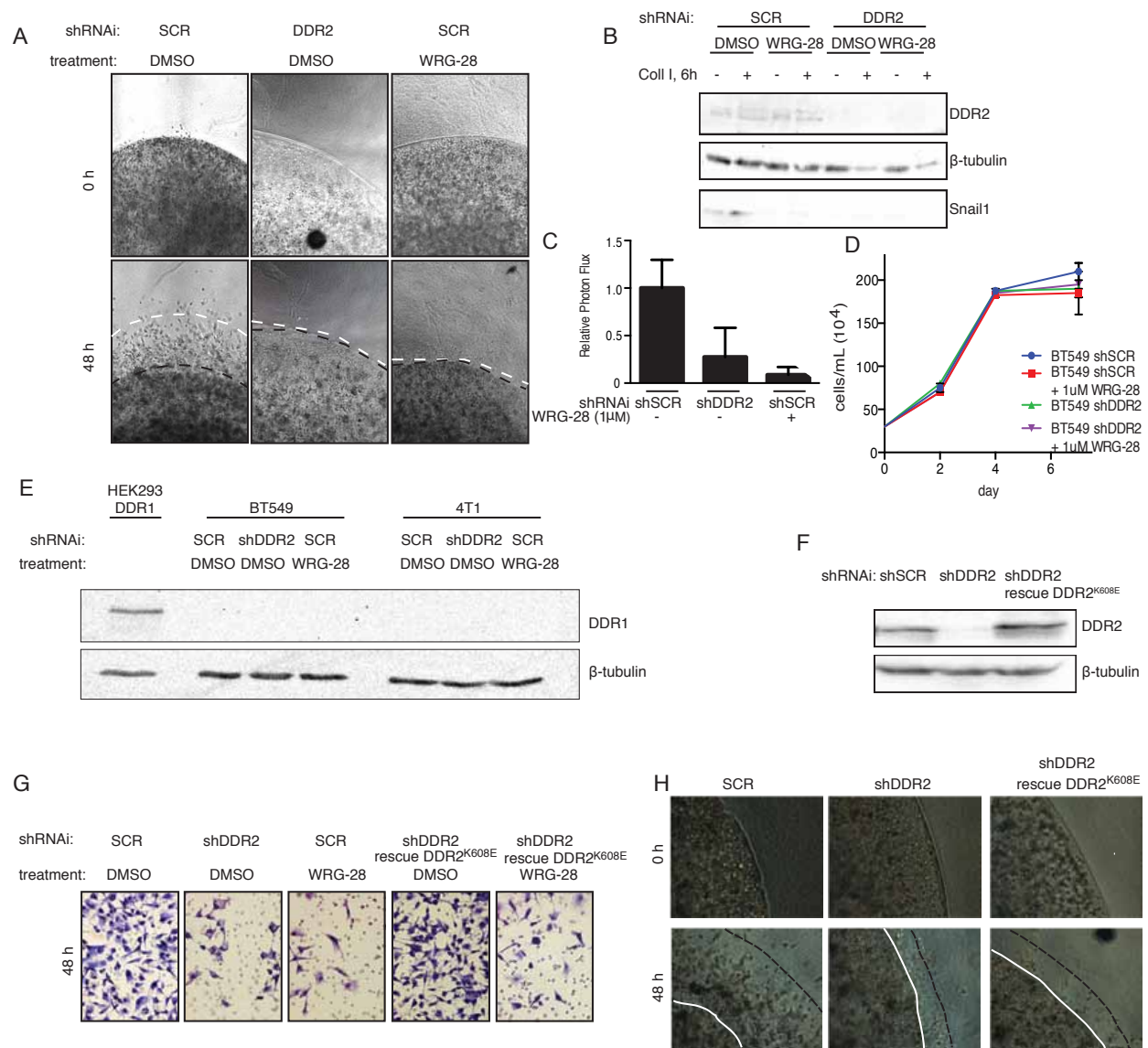


Fig. S5. (A) BT549 cell migration in 3D collagen I gels treated with 1 μ M WRG-28 or control, compared to cells depleted of DDR2. Representative images shown. Black dashed line delineates original cell cluster boundary, white dashed line delineates the invasive front at 48h. (B) 4T1 cells added to collagen I coated (2mg/mL) or uncoated plates in the presence of WRG-28 (1 μ M) or DMSO for 6 hours. Western blots were performed for analysis of SNAIL1 stabilization. (C) Matrigel invasion of 4T1-GFP-luc cell lines treated with 1 μ M WRG-28 or control as compared to depleted of DDR2 at 48 hours. Invasion measured by bioluminescence of cells on fluoroblock transwell inserts. Mean \pm SEM. (n=3 per condition). (D) Proliferation of BT549 control or shDDR2 depleted cells in the presence or absence of 1 μ M WRG-28. (E) Western blot of BT549 and 4T1 cells treated with 1 μ M WRG-28 or control, compared to cells shRNAi-depleted of DDR2 were performed for analysis of DDR1 expression. HEK293 cells expressing a DDR1-Myc plasmid were used as a control for DDR1 expression (F) BT549 cells depleted of DDR2 (shDDR2) were infected with lentivirus expressing a kinase dead DDR2 (DDR2K608E). Western blot analysis was performed to confirm re-expression of DDR2. (G) Matrigel invasion of BT549 cell lines treated with 1 μ M WRG-28 or control, compared to cells shRNAi-depleted of DDR2 or depleted cells rescued with kinase dead DDR2 (DDR2K608E) at 48 hours. Representative images of H&E stained inserts. (H) Cell migration in 3D collagen gels of BT549 cells as compared to cells depleted of DDR2, or depleted cells rescued with a kinase dead DDR2 (DDR2K608E). Distance traveled relative to control cells was determined at 48hrs. Representative images shown. Solid white line delineates original cell boundary, dashed black line delineates invasive front.

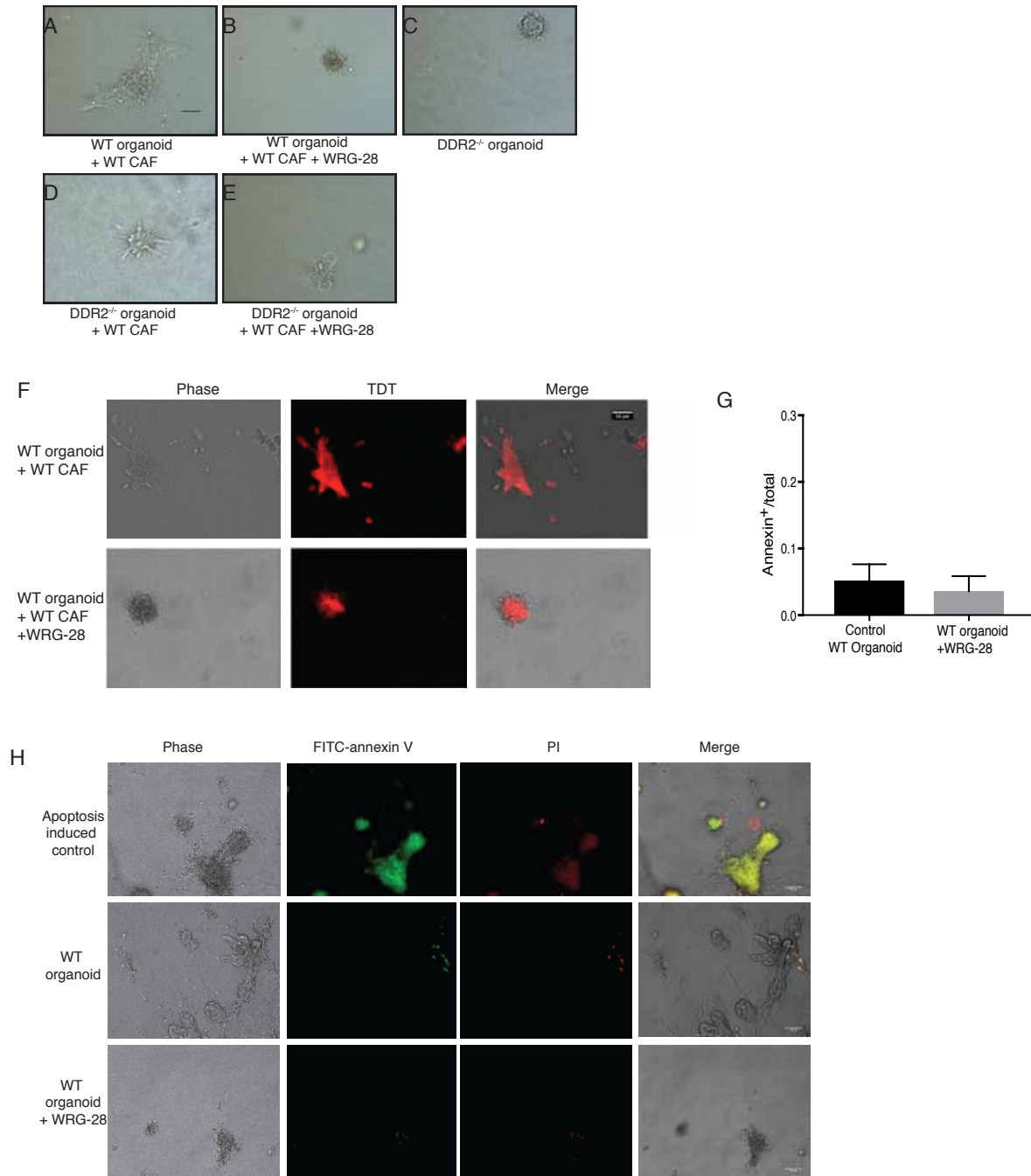


Fig. S6. (A-E) Representative images of scored tumor organoids: (A) invasive WT organoid in the presence of WT CAFs, (B) WT organoid in the presence of WT CAFs and 1 μ M WRG-28, (C) non-invasive Ddr2^{-/-} organoid, (D) Invasive Ddr2^{-/-} organoids in the presence of WT CAFs, (E) Ddr2^{-/-} organoid in the presence of WT CAFs and 1 μ M WRG-28. Scale bar=100 μ m. (F) Phase contrast image, Tomato fluorescence of MMTV-PyMT; Ddr2^{+/+}; ROSA-LSL-TdTomato tumor organoids, and merged image confirming that invasive foci contain migrating tumor cells. Scale bar = 50 μ m. (G) Quantification of positive annexin V staining as compared to total organoid area for control WT organoids or WT organoids treated with 1 μ M WRG-28. (H) Representative images of phase, PI staining, and annexin V staining of organoids quantified in (B). Doxorubicin induced apoptosis was used as a positive control of staining. Scale bar = 50 μ m

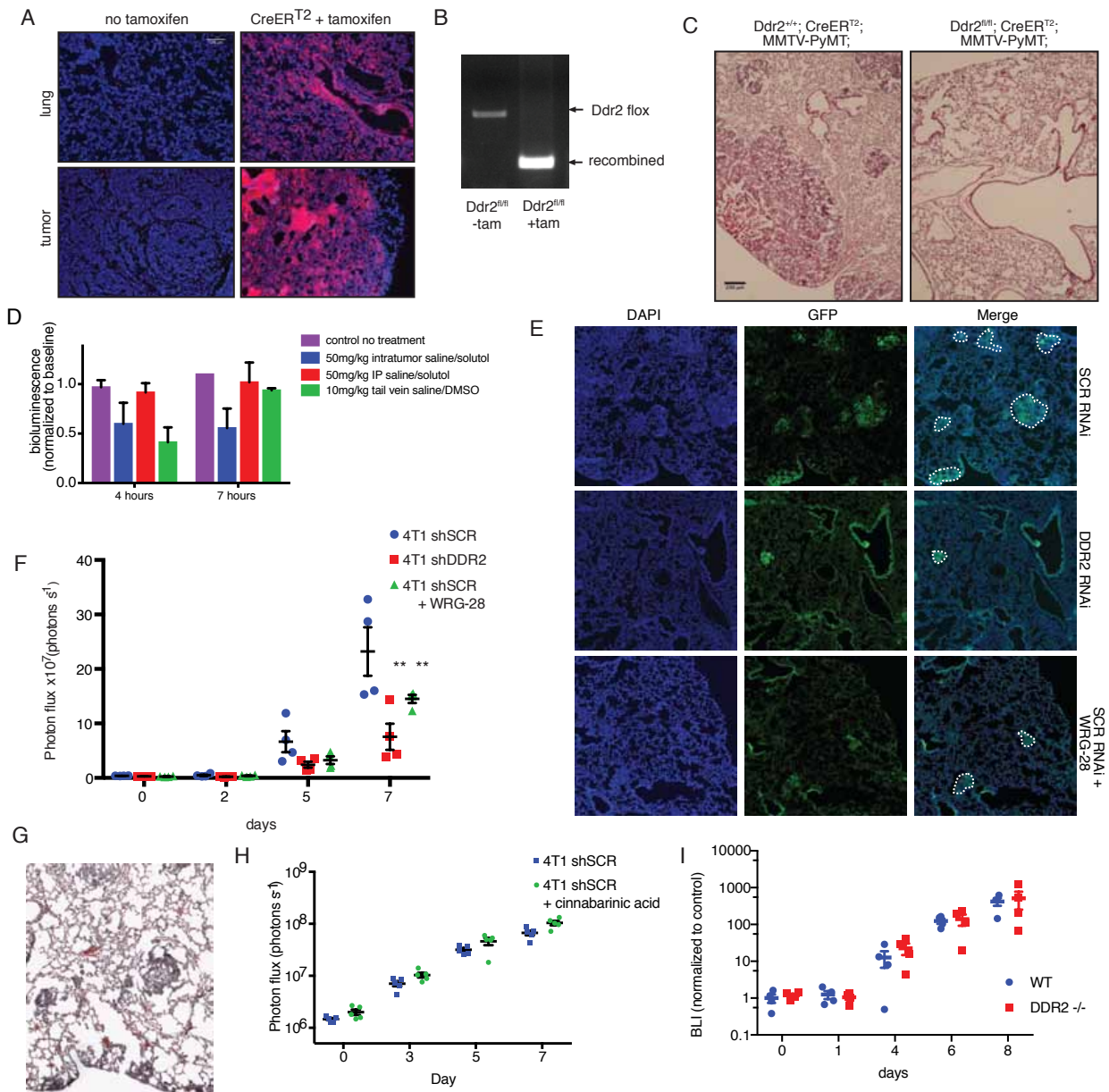


Fig. S7. (A) Tomato (red) staining of mammary tumor/lung sections from *Ddr2^{fl/fl}; CreERT²; MMTV-PyMT* mice \pm tamoxifen (Tam) administration. DAPI (blue) staining of nuclei. Scale bar=100 μ m. (B) DNA PCR detection of floxed and recombined *DDR2* allele from a mouse prior to or after Tam administration (tumor at endpoint). (C) Representative images of lungs from indicated mice analyzed in Figure 4C. Scale bar=200 μ m. (D) 4T1-Snail-CBG tumor bearing mice at timepoints following treatment with WRG-28. WRG-28 was administered at indicated doses, which represent the maximum solubility in the tested excipient. Quantification of relative bioluminescence is shown as compared to pre-treatment baseline. Mean \pm SEM (E) Representative histologic images of GFP expressing tumor nodules in lungs of mice quantified in Fig. 5E. Dashed white line delineating GFP positive tumor foci that were quantified. (F) Bioluminescence quantification from second cohort of tail vein metastasis assay, BALB/cJ mice injected with 4T1 GFP-luc expressing cells. Means \pm SEM; data derived from one experiment of four mice per condition. ** $p < 0.01$, two way ANOVA. (G) H&E staining of a serial section of SCR RNAi in Figure S7E illustrating consistency between GFP signal and tumor foci. (H) BALB/cJ mice are injected by tail vein with 5×10^5 4T1-GFP-luc expressing cells: control (shSCR) and mice injected with control cells and treated daily with cinnabarinic acid (inactive against *DDR2*) control (blue circles), cinnabarinic acid treated (green squares). Mean \pm SEM; data derived from one experiment of five mice per condition. (I) C57BL/6 mice wild type or *DDR2* global null (*DDR2*^{-/-}) injected by tail vein with 5×10^5 Bo1-GFP-luc expressing cells

Supplemental Experimental Procedures

Synthesis and Chemical features of WRG-28

4-(bromomethyl)-*N*-ethylbenzenesulfonamide.

Adapted from (1). To ethylamine HCl (120mg, 1.5 mmol) and triethyl amine (0.3mL, 2.2mmol) in CH₂Cl₂ (15mL) under inert gas at 0°C, 4-bromomethyl benzene sulfonyl chloride (300mg, 1.1mmol) dissolved in CH₂Cl₂ was added dropwise. Reaction brought to room temperature and stirred overnight. An additional 15mL CH₂Cl₂ was added, and washed with water (3 x 25mL), brine (1x25mL), and dried over Na₂SO₄. Solvent was removed under reduced pressure, and the resulting 4-(bromomethyl)-*N*-ethylbenzenesulfonamide used without further purification.

N-ethyl-4-(((3-oxo-5a,10a-dihydro-3*H*-phenoxazin-7-yl)oxy)methyl)benzenesulfonamide
4-(bromomethyl)-*N*-ethylbenzenesulfonamide (50mg, 0.2mmol), resorufin sodium salt (42mg, 0.2mmol), and CsCO₃ (88mg, 0.27mmol) in DMF (15mL) were heated to 100°C overnight with stirring. EtOAc (50mL) was added and resulting organic solution washed extensively with water. After drying over Na₂SO₄, solvent was removed under reduced pressure. Resulting product was purified by silica chromatography (hexane:EtOAc) to afford *N*-ethyl-4-(((3-oxo-5a,10a-dihydro-3*H*-phenoxazin-7-yl)oxy)methyl)benzenesulfonamide as an orange solid.

¹HNMR (400 MHz, CDCl₃): δ 7.94 ppm (dd, 2H), 7.76 (dd 1H), 7.62 (dd 2H), 7.45 (dd, 1H), 7.05 (t, 1H), 6.9-6.85 (m, 2H), 6.35 (s, 1H), 5.27 (s, 2H), 4.38 (s, 1H), 3.08 (q, 2H), 1.16 (t, 3H).
HRMS for C₂₁H₁₈N₂O₅S₁ [M+H]⁺: m/z = 411.2

Cell culture and viral infections

HEK293, HEKEBNA and HEK293T cells were from ATCC. MCF-10A cells were provided by L. Michel (Washington University in St Louis, USA). BT549 cells were provided by J. Weber (Washington University in St. Louis, USA). Bo1-Luc-GFP cells were provided by S. Stewart (Washington University in St. Louis, USA). 4T1- Luc-GFP cells were described previously(2). Production of lentiviruses and infection of target cells were described previously(2). To make stable cell lines of BT549 and 4T1 cells selection was carried out in 3 µg/ml puromycin.

Reagents

Triple helical collagen binding peptides GPC(GPP)₅-GPRGQOGVNIeGFO-(GPP)₅GPC-NH₂ and GPC(GPP)₅-GFOGER-(GPP)₅GPC-NH₂ were purchased from Richard Farndale (University of Cambridge, UK). α1β1 integrin, DDR1-Fc and DDR2-myc/His were purchased from R&D systems. DDR2-Fc was purchased from Creative Biomart.

Plasmids, shRNAi lentiviruses

pFLR DDR2-Flag and pFLR SNAIL1.CBG plasmids and DDR2 shRNAi were previously described(2). pCEP-His-DDR2, pc-DDR1-Fc and pc-DS2-Fc plasmids were provided by Birgit Leitinger(3, 4) (Imperial College London, UK). pCDNA3.1 DDR1-myc was provided by Rafael Fridman (Wayne State University, USA). For mutation studies of full length receptor, the cDNA of DDR2 was subcloned into pcDNA3.1-myc plasmid. Overlapping PCR was used to introduce point mutations and then subcloned back into pcDNA3.1. Plasmids for recombinant DDR2 protein were constructed by removing the N-terminal His and Myc tags from pCEP-His-DDR2 ECD and using PCR to introduce a C-terminal His tag to DDR2 (amino acids Lys²² to Thr³⁹⁸). BM-40 signal sequence was maintained at the N-terminus. For point mutants, overlapping PCR was used to introduce point mutations and then subcloned back into the pCEP-pu vector. For DDR2^{K608E} plasmid, overlapping PCR was used to introduce the point mutation, and then subcloned into the pFLRu vector(5) with a YFP tag. All mutations and cloning were verified by sequencing. shRNAi were subcloned into the pFLRu vector. shRNAi target sequences are as follows: SCR control sequence 5'-CCTAAGGTTAAGTCGCCCTCGCTC-3', shDDR2 5'-

GCCAGATTTGTCCGGTTCATT-3'. For rescue experiments, a shDDR2 directed at the 3' UTR with sequence 5'- GCCCATGCCTATGCCACTCCAT-3' was used to allow for expression of rescue construct.

Solid Phase Collagen Binding Experiments

Collagens or collagen peptides (100uL) were diluted in 0.01 N acetic acid coated onto Immulon 2 HB 96-well plates (Fisher Scientific) overnight at 4°C. Collagen binding peptides have been previously validated and described in detail(6, 7). For DDR proteins, the collagen peptide included the binding sequence GPRGQOGVNleGFO. For integrin $\alpha1\beta1$, the collagen peptide included the binding sequence GFOGER. Wells were then blocked for 1 h at room temperature with 1 mg/ml bovine serum albumin in phosphate-buffered saline plus 0.05% Tween 20. Recombinant proteins, diluted in incubation buffer (0.5 mg/ml bovine serum albumin in phosphate-buffered saline plus 0.05% Tween 20), were added for 3 h at room temperature. Wells were washed with incubation buffer between all incubation steps. Bound DDR2-His protein or $\alpha1\beta1$ -His were detected with anti-His conjugated HRP monoclonal antibody (1:2500 dilution), added for 1 h at room temperature. Bound DDR1-FC or DS2-Fc protein were detected with goat anti-human Fc coupled to horseradish peroxidase (1:2500 dilution), added for 1 h at room temperature. Detection was achieved using o-phenylenediamine dihydrochloride (Sigma), added for 3–5 min. The reaction was stopped with 3M H₂SO₄, and plates were read in a 96-well plate reader at 492 nm. $\alpha1\beta1$ integrin assay was performed as described(8), but with anti-His conjugated HRP used for detection.

Peptide labeling

NHS-fluorescein (Thermo scientific) was used to label collagen toolkit peptide. Labeling was carried out at a 5 fold molar excess of labeling reagent to peptide on ice for 2 hours. Non-reacted NHS-fluorescein was removed by dialysis, and the resulting labeled peptide lyophilized and then resuspended. Solid phase assay was used to confirm there was no loss of DDR2 binding upon conjugation of the peptide.

Peptide plating quantification

Increasing amounts of fluorescein conjugated collagen peptide were plated in triplicate into wells of a Immulon 2HB plate. Plating was carried out overnight at 4°C. At that time, fluorescence intensity of each well was detected using a Tecan Infinite 200 PRO plate reader. Wells were then washed 3 times with PBS, and post wash fluorescence intensity was measured to determine the portion of the plated peptide that was adsorbed onto the plate.

Biolayer Interferometry

Biolayer Interferometry (BLI) with an Octet (ForteBio, Menlo Park, CA) instrument was used to assess WRG-28 binding to various protein constructs. DDR2 was randomly biotinylated *in vitro* using EZ-link NHS-PEG4-Biotin (Thermo Scientific) at a 1:2 molar ratio (protein: reagent). Streptavidin-coated biosensors (ForteBio) were used to capture biotinylated DDR2 onto the surface of the sensor. After reaching baseline, sensors were moved to association step for 600 s and then dissociation for 300 s. Curves were corrected by referencing technique using both biotin-coated pins dipped into the experimental wells. The binding buffer was identical to that of the solid phase assay.

Column Calibration

A molecular weight calibration curve for the Superdex 200 10/300 GL column was established using GE Gel Filtration Calibration Kit HMW following manufacturer's instructions. PBS was used to solubilize the standard protein samples.

Size exclusion chromatography

Size exclusion chromatography was carried out at 4°C using a BioRad Biologic Duoflow system equipped with a Superdex 200 Increase 10/300 GL column (GE). Experiments were run using PBS at a 0.5mL/min flow rate and elution monitored at UV absorbance 280nm. 25µg of protein were incubated in solution with 1µM WRG-28 or DMSO for 1 hour, then injected, and 1mL fractions were collected upon elution. Fractions were concentrated using Vivaspin 500 centrifugal concentrators (10K MWCO), and run on 10% gel under non-reducing conditions. To assess of collagen binding of various fractions, they were immediately spin concentrated, protein concentration determined, and normalized across samples. Samples were then subjected to binding in the solid phase plate assay.

Cell Surface Biotinylation

Cell surface biotinylation was used to confirm cell surface expression of protein constructs. HEK293 cells expressing the indicated constructs were incubated with cell impermeable EZ-link NHS-PEG4-Biotin in PBS for 30 minutes on ice. Cells were then washed twice with 100mM glycine in PBS to quench reaction. Cells were lysed, and the expressed constructs immunoprecipitated using the indicated protein tag. Lysates were run and analyzed by SDS-PAGE, blotting with Streptavidin-HRP to detect biotin. Blots were stripped and reprobed for the indicated protein to confirm band identity. Non-biotin treated lysates were run as a control.

Assessment of receptor dimerization

Dimerization was asses by chemical cross linking analysis. HEK293 cells expressing the indicated constructs were treated with 0.1M BS³ (Thermo Scientific) in PBS for 30min at room temperature, after which the reaction was quenched with 15mM glycine. Cells were then lysed and lysates analyzed by SDS-PAGE.

Molecular docking

The homology model of the DDR2 extracellular domain was created by using SWISS-MODEL protein structure homology modeling server(9). PDB 4AG4 was used as a template. For docking studies, PyRx using the AutoDock Vina Wizard(10) was used. For molecular visualization, docking poses generated by Autodock Vina were loaded into Pymol.

Membrane Fractionation

Cell homogenate was prepared using homogenization buffer (250 mM sucrose, 1 mM EDTA, 10 mM Tris HCl buffer, pH 7.2 plus protease inhibitors) and then briefly sonicated. Intact cells, nuclei and cell debris were removed by centrifugation of the homogenate at 500 x g for 10 minutes at 4°C. Pellet was discarded. The remaining solution was centrifuged at 100,000 x g for 1 hour at 4°C. The supernatant at this point was considered the soluble cytosolic proteins. The remaining pellet was washed with homogenization buffer and recentrifuged at 100,000 x g, 4°C, for 1 hour. Supernatant was discarded. The remaining pellet containing membrane fraction was solubilized with sample buffer, and all fractions were analyzed by SDS-PAGE, using the indicated controls

Immunoprecipitation and western blots.

For collagen dependent phosphorylation, indicated concentrations of collagen I in 0.01N acetic acid were plated for 1hr at 37°C. plates were washed twice with PBS, and cells then plated in culture medium. Cells were lysed with a non-denaturing lysis buffer as described previously(2). Five hundred micrograms of whole-cell lysate, as determined by Bradford analysis (BioRad), was used for immunoprecipitation. Blots were probed with indicated antibodies, followed by corresponding horseradish peroxidase-conjugated secondary antibodies. Detection was preformed using SuperSignal Chemiluminescent substrate (Thermo Scientific) on a ChemiDoc

XRS+(BioRad). Integrated relative densities of individual bands were quantified using ImageLab software. All quantification was performed under conditions of linear signal response.

RTK Signaling Array

MCF10A cells were starved overnight, and then stimulated with media containing 20% horse serum + EGF for 5, 15, or 60 minutes in the presence or absence of indicated concentrations of WRG-28. Cells were lysed, and lysates were assayed using PathScan RTK signaling array (Cell Signaling) or Proteome Profiler Human Phospho-RTK Array (R&D systems). Following detection on a ChemiDoc XRS+(BioRad), integrated relative densities of individual dot blots were quantified using ImageLab software, and normalized to positive blot controls. All quantification was performed under conditions of linear signal response.

Cell proliferation analysis

Cells were seeded at 3×10^4 cells per well in triplicate in 24 well plates in 500 μ L growth medium on day 0. Cells were trypsinized, resuspended in a total volume of 500 μ L of medium and counted with a haemocytometer at the intervals shown.

Migration and Invasion Assays

For 3D cell migration assays, 10^5 cells were embedded in 20 μ L of type I collagen gel (2.0mg/mL) extracted from rat tail (BD Biosciences). After gelling, the plug was embedded in a cell-free collagen gel (2.0 mg/mL) within a 24-well plate. After allowing the surrounding collagen matrix to gel (1 h at 37°C), 0.5 mL of culture medium was added on the top of the gel and cultured for another 2 days. Invasion distance from the inner collagen plug into the outer collagen gel was quantified. For invasion assays, Transwell cell invasion assays were performed using either 24-well polycarbonate membrane (Corning) with 8- μ m pore size, or 24-well FluoroBlok Transwell insert (BD) with 8- μ m pore size. Inserts were prepared by coating the upper surface with 1 mg/mL of Matrigel (BD Biosciences) for 4–6 h at 37°C in a 5% CO₂ incubator. 5×10^4 BT549 or 4T1-Luc cells in DMEM containing 1% FBS were seeded into the upper chamber of the insert. The bottom chamber contained DMEM with 10% FBS. After 24 or 48 hr, Membranes were processed. Polycarbonate membranes were stained with HEMA3 staining kit (Fisher) and then mounted and enumerated based on number of cells per 20x high power field, 5 fields per insert. For FluoroBlok transwells, luminescence intensity was measured using a FluoStar Optima microplate reader (BMG Labtech) for 10 individual fields on the bottom of each insert.

Tumor Organoid and CAF coculture

Isolation of tumor organoids and CAFs was described previously(11). Primary tumor organoids (30–50, each 200–1,000 cells) with or without CAFs (750 cells) were cultured in 50 μ L droplets of 3mg/mL acid-solubilized rat-tail collagen I (BD Biosciences), and number of invasive organoids were enumerated daily for 4 days. Organoids were scored as invasive if they contained ≥ 1 protrusive projection.

Organoid Apoptosis Staining

Organoids derived from MMTV-PyMT tumor bearing mice were grown in 3D collagen culture as indicated in experimental methods. Organoids were grown in the presence of control DMSO or 1 μ M WRG-28. On day 4, positive control wells were treated with 1 μ M doxorubicin for 4 hours to induce apoptosis. Organoids were then stained using an annexin V-FITC/PI apoptosis detection kit (Abcam), and imaged. 10 organoids/condition were imaged, and percent of organoids staining positive for annexin V was quantified using ImageJ software.

Animal Studies

All procedures and care of animals were done in accordance with a protocol approved by the Washington University Institutional Animal Care and Use Committee (St. Louis, MO), and were performed in accordance with institutional and national guidelines.

Temporal deletion of *Ddr2*. *Ddr2^{fl/fl}*; ROSA-LSL-TdTomato or *Ddr2^{+/-}*; ROSA-LSL-TdTomato mice were crossed to MMTV-PyMT; ROSA-CreER^{T2} mice. At 8 weeks, experimental and control mice were switched to 400 citrate tamoxifen-supplemented non-pelleted dry feed (Envigo) for 2 weeks. The tumor bearing mice were monitored weekly and euthanized when the largest tumor reached 2 cm in diameter. Lungs were fixed overnight in 10% formalin, cryopreserved in 30% sucrose overnight, and finally embedded in OCT and frozen in a dry ice/ethanol bath. Frozen specimens were sectioned with a cryostat (6 μ m) and analyzed by fluorescence microscopy for tomato expression or stained with haematoxylin and eosin for histological analysis. For analysis of lung metastasis, microscopically visible metastatic foci were counted from three H&E stained sections taken 200 μ m apart and reported as the total number of metastases in those three sections.

Breast implant in vivo assay. Eight-week old female BALB/cJ mice (Jackson Labs) were anaesthetized with a ketamine/xylazine cocktail (90 mg/kg ketamine and 13 mg/kg xylazine, intraperitoneal injection) and the abdomen was sterilized using povidone-iodine (Betadine) solution and ethanol. A small Y-shaped incision was made in the lower abdominal skin to expose the fourth mammary gland using surgical scissors and bleeding vessels were cauterized. 4T1-Snail.CBG cells (1×10^6) in 50 μ L DMEM were injected into the fourth mammary gland using a 29-gauge needle. The skin flaps were replaced and closed using 9 mm wound clips, and the surgical site was swabbed with triple-antibiotic cream. When tumors were 1 cm in diameter, in vivo biochemical response studies were conducted by bioluminescence imaging (BLI) at baseline, followed by IV lateral tail vein injection of either control saline, or indicated doses of WRG-28 in saline/DMSO, and BLI at indicated time points. The baseline BLI signal for each mouse served as its own control.

For lung metastasis formation assay, 5×10^5 cells in 100 μ L DMEM were injected into the lateral tail vein of BALB/cJ mice. Beginning on day 0, mice were treated with either control saline, or 10 mg/kg WRG-28 in saline/DMSO daily for 7 days, and BLI imaging used to follow tumor growth at time points indicated. After 7 days, mice were euthanized and lungs removed and fixed in 10% formalin for 24 h, cryopreserved in 30% sucrose overnight, and finally embedded in OCT and frozen in a dry ice/ethanol bath. Frozen specimens were sectioned with a cryostat (6 μ m) and analyzed by fluorescence microscopy for GFP expression or stained with haematoxylin and eosin for histological analysis.

To test the contribution of stromal DDR2 in the lung colonization assay, global deletion of DDR2 in C57BL/6 mice was achieved by backcrossing a previously generated DDR2-null allele(11) in C57BL/6 mice for 10 generations. Heterozygote crosses generated DDR2 +/+ (wild type) and DDR2 -/- (null) mice for the experiment. Bo1-GFP-luc cells, a C57BL/6 derived mouse breast tumor line that is known to metastasize to lung(12), were injected into the lateral tail vein (5×10^5 cells in 100 μ L DMEM) and BLI imaging used to follow tumor growth at the time points indicated. For all BLI, mice were anaesthetized with isoflurane and imaged using the IVIS 100 bioluminescent imaging system (Perkin Elmer) following an intraperitoneal injection of d-luciferin (150 mg/kg).

Statistics

All data represent the mean \pm SEM of the indicated number of experiments. Statistical

parameters and IC₅₀ values were calculated using Prism. Statistical significance was calculated by the indicated test, considering p<0.05 as statistically significant.

Supplemental References

1. Zidar N, *et al.* (2011) New 5-benzylidenethiazolidin-4-one inhibitors of bacterial MurD ligase: design, synthesis, crystal structures, and biological evaluation. *European journal of medicinal chemistry* 46(11):5512-5523.
2. Zhang K, *et al.* (2013) The collagen receptor discoidin domain receptor 2 stabilizes SNAIL1 to facilitate breast cancer metastasis. *Nature cell biology* 15(6):677-687.
3. Leitinger B (2003) Molecular Analysis of Collagen Binding by the Human Discoidin Domain Receptors, DDR1 and DDR2. *The Journal of biological chemistry* 278(19):16761-16769.
4. Xu H RN, Stathopoulos S, Myllyharju J, Farndale RW, Leitinger B (2011) Collagen binding specificity of the discoidin domain receptors: Binding sites on collagens II and III and molecular determinants for collagen IV recognition by DDR1. *Matrix Biology* 30:16-26.
5. Feng Y, *et al.* (2010) A multifunctional lentiviral-based gene knockdown with concurrent rescue that controls for off-target effects of RNAi. *Genomics, proteomics & bioinformatics* 8(4):238-245.
6. Raynal N, *et al.* (2006) Use of synthetic peptides to locate novel integrin alpha2beta1-binding motifs in human collagen III. *The Journal of biological chemistry* 281(7):3821-3831.
7. Carafoli F, *et al.* (2009) Crystallographic insight into collagen recognition by discoidin domain receptor 2. *Structure* 17(12):1573-1581.
8. Knight CG, *et al.* (2000) The collagen-binding A-domains of integrins alpha(1)beta(1) and alpha(2)beta(1) recognize the same specific amino acid sequence, GFOGER, in native (triple-helical) collagens. *The Journal of biological chemistry* 275(1):35-40.
9. Guex N, Peitsch MC, & Schwede T (2009) Automated comparative protein structure modeling with SWISS-MODEL and Swiss-PdbViewer: a historical perspective. *Electrophoresis* 30 Suppl 1:S162-173.
10. Trott O & Olson AJ (2010) AutoDock Vina: improving the speed and accuracy of docking with a new scoring function, efficient optimization, and multithreading. *Journal of computational chemistry* 31(2):455-461.
11. Corsa CA, *et al.* (2016) The Action of Discoidin Domain Receptor 2 in Basal Tumor Cells and Stromal Cancer-Associated Fibroblasts Is Critical for Breast Cancer Metastasis. *Cell reports* 15(11):2510-2523.
12. Ross MH, *et al.* (2017) Bone-Induced Expression of Integrin beta3 Enables Targeted Nanotherapy of Breast Cancer Metastases. *Cancer research* 77(22):6299-6312.